

## CONTRASTING SIZE DISTRIBUTIONS OF CHONDRULES AND INCLUSIONS IN ALLENDE CV3.

Kent. R. Fisher<sup>1</sup>, Alastair W. Tait<sup>2</sup>, Justin I. Simon<sup>3</sup>, <sup>4</sup>Jeff N. Cuzzi. <sup>1</sup>University of Cincinnati, Cincinnati, OH, 45219, <sup>2</sup>Monash University, Clayton, Vic., 3800, Australia, <sup>3</sup>Center for Isotope Cosmochemistry and Geochronology, ARES, NASA Johnson Space Center, Houston, TX 77058, USA (Justin.I.Simon@NASA.gov), <sup>4</sup>NASA Ames, Moffett Field, CA 94035, USA (jeffrey.cuzzi@nasa.gov).

**Introduction:** There are several leading theories on the processes that led to the formation of chondrites, e.g., sorting by mass [1,2], by X-winds [3], turbulent concentration [4], and by photophoresis [5]. The juxtaposition of refractory inclusions (CAIs) and less refractory chondrules is central to these theories and there is much to be learned from their relative size distributions. There have been a number of studies into size distributions of particles in chondrites but only on relatively small scales primarily for chondrules, and rarely for both CAIs and chondrules in the same sample (e.g. [6-17]). We have implemented macro-scale (25 cm diameter sample) and high-resolution micro-scale sampling of the Allende CV3 chondrite to create a complete data set of size frequencies for CAIs and chondrules.

**Methods:** As part of an ongoing study to characterize nebular components in carbonaceous chondrites, CAIs and chondrules were characterized in X-ray phase maps obtained by scanning electron imaging (SEM) for seven Allende samples (including 0.50 cm<sup>2</sup>, 0.68 cm<sup>2</sup>, 0.70 cm<sup>2</sup>, 0.77 cm<sup>2</sup>, 0.72 cm<sup>2</sup>, 0.79 cm<sup>2</sup>, 0.80 cm<sup>2</sup> sized pieces; 2 that were new and from a region of Allende from which a large (~ 25 cm) slab had previously been characterized [18] and 5 that were obtained previously by [19]). The SEM data were then combined with a representative section of the ~25 cm slab. The SEM data allow for accurate phase recognition and size characterization at the smallest sizes and the large size of the slab allows analysis at a much larger length scales. The latter should result in a better representation of larger CAIs, whose feature may not be fully apparent from studies of smaller samples.

**Data Preparation.** To create an accurate representation of the CAI and chondrule size distributions at smaller and larger scales, analyses of images of different scales were needed. Samples were imaged by SEM at a resolution of 3.34  $\mu\text{m}/\text{pixel}$  to produce element maps for further CAI and chondrule identification. These SEM images were separately digitized by 4 researchers. The mosaic image (referred to as 'macro-scale') was also digitized to gather data on the larger CAIs that may not be fully represented in any of the 7 micro-samples.

**Image Analysis.** Digitized images were run through ImageJ and filtered at a confidence level of  $>80,000 \mu\text{m}^2$  for CAIs. Digitized SEM images, including the mosaic image were run through ImageJ without filtering. All images were analyzed in ImageJ by the

same process with the exception of the smallest, difficult to identify sizes in the macrophotography.

The large slab sample was extensively imaged at a resolution of 13.88  $\mu\text{m}/\text{pixel}$ . Both sides (one designated 'LH' and the other designated 'RH') were imaged by macrophotography and mosaic images were created using Adobe Illustrator. All image files were aligned so that each of the ~400 individual image files was in the same orientation. The mosaic images were divided into 9 equal size sections of ~1,000,000,000  $\mu\text{m}^2$  to facilitate easy comparison to other samples and other studies. Four researchers separately digitized CAIs and chondrules in each section.

**Compiling of Data.** Frequency analysis was completed for the ImageJ results for each set of images (SEM and macro). The frequency data sets were merged to create an accurate size distribution of the Allende CAIs and chondrules. The SEM data and macro data were scaled up and down, respectively, to produce distributions on a ~1,000,000,000  $\mu\text{m}^2$  scale in order to compare with the micro data. After some iteration, it was determined that the best merging point for the SEM and macro data would be at the 225  $\mu\text{m}$  (major axis) size limit. Particle size distributions below 225  $\mu\text{m}$  were calculated from the SEM images while everything above was calculated using the macro images.

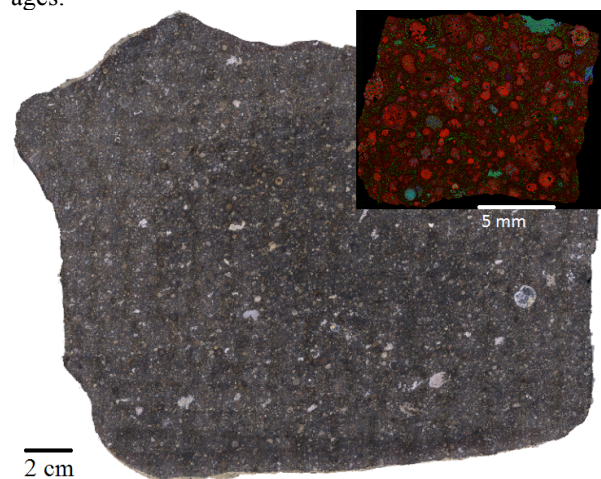


**Figure 1.** Representative images of studied samples: (main) The 'RH' Allende slab under plain light. (inset) SEM false-colored phase X-ray map; Mg=red, Al=blue, Ca=green. Note different scales.

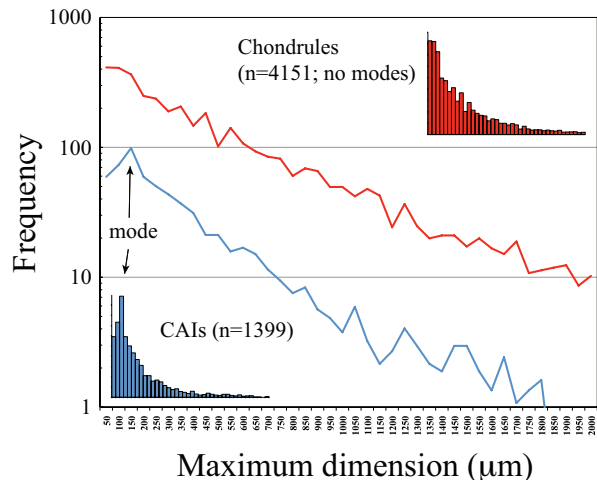


**Figure 2.** Log plot showing size distributions for chondrules (red) and CAIs (blue) using data compiled from SEM and macrophotography of Allende CV3. X-axis tick marks are 50  $\mu\text{m}$  intervals. A prominent mode can be seen in the CAI data (histogram, lower left inset) while the chondrules display a continuous function (histogram, upper right inset).

*Chondrule Fragments.* One concern with the SEM chondrule data is the presence of chondrule fragments. Chondrules are known to be originally of approximately spherical shape and even when slightly deformed they likely retain their round dimensions. Many polygonal shaped chondrule fragments were seen at the SEM scale, but few that were obviously fractured. These fragments can be filtered out of the chondrule data by measuring the circularity of all the chondrules recorded and then excluding any chondrule with circularity less than 0.55. Figure 3 shows circularity versus major axis plot of all the chondrules and CAIs recorded in the SEM images.

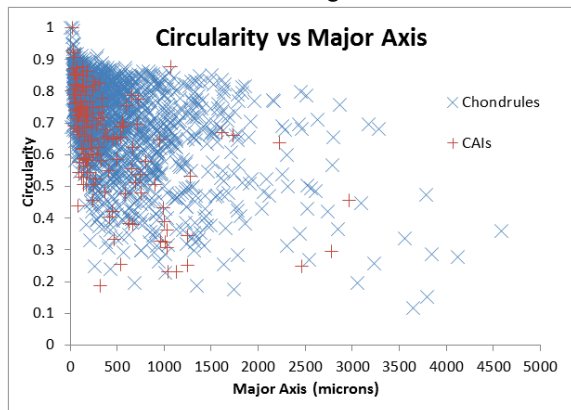


**Figure 3.** Scatterplot showing circularity (y-axis) versus major axis length (x-axis) for chondrules and CAIs. Chondrules are designated by blue X and CAIs are designated by red +. ImageJ defines circularity as  $= 4\frac{1}{4} \times \text{area}/\text{perimeter}^2$ .

**Discussion:** Two issues must be considered when making inferences from these analyses. First, it is assumed that the inclusions were cut non-diametrically

and therefore may not accurately represent the actual sizes of CAIs and chondrules in Allende. However, these data are a good representation of the relative length frequency of the long axes of CAIs and chondrules in a standard size area of  $\sim 1,000,000,000 \mu\text{m}^2$ .

Second, there is the possibility that the particles underwent some sort of deformation [19], which would affect the sizes. If this deformation was equal across the parent body then the comparisons should still be accurate.

**Conclusions:** Several potentially important findings arise from comparing CAIs and chondrule populations in Allende: (1) that CAIs exhibit a mode at approximately 150-200  $\mu\text{m}$  whereas chondrule sizes appear to drop exponentially, (2) the largest chondrules are at least as large as the largest CAIs, and (3) regardless of whether chondrule data are filtered for circularity, the size distribution is roughly the same, which suggests that at least some of the smallest chondrules are not actually fragments.

**Future Work:** These data sets will be processed by matrix inversion to transform 2-D particle section areas into volumes (i.e., unfolded, [18]) to get a more accurate particle size distribution. Any such integration will require proper scaling, which is still being worked out. The methods of data analysis for this study were created with the idea that inclusion size data (preferably ImageJ outputs) could be inserted and size distribution analysis produced with minimal work allowing for easy comparisons of different carbonaceous chondrites.

**Acknowledgement:** This work could not have been completed without the generous loan of the  $\sim 25$  cm slab sample from the personal collection of Joseph Minafra and a similar adjacent slab from the personal collection of Phil Mani.

**References:** [1] Teitler S. A. et al. (2010) *MPS*, 45, 1124-1135. [2] Cuzzi, J. N. et al. (2001) *APJ*, 546, 496-508. [3] Shu F. H. et al. (1996) *Science*, 271, 1545-1552. [4] Hogen R. C. et al. (1999) *Physical Rev. E*, 60, 1674-1680. [5] Wurm G. & Krauss O. (2006), *Icarus*, 180, 487-495. [6] McSween, H.Y. (1977) 41, 1777-1790. [7] Kornacki, A.S. and J.A. Wood (1984) 89, B573-B587. [8] Rubin, A.E., (1998) *Meteoritics and Planetary Sciences* 33, 385-391. [9] Scott, E.R.D., S.G. Love, and A.N. Krot, 1996, Cambridge University Press: Cambridge. 87-96. [10] Brearley, A.J. and R.H. Jones, 1998, *Mineralogical Society of America: Washington, D.C.* 1-398. [11] Norton, M.B. and H.Y.J. McSween (2007). *38th LPSC 1807*. [12] Dodd, R.T., *EPSL*, 1976. 30, 281-291. [13] Hughes, D.W., *EPSL* 1978. 38, 391-400. [14] Hughes, D.W., *EPSL* 1978. 39, 371-376. [15] Rubin, A.E., *Meteoritics*, 1989. 24: p. 179-189. [16] Rubin, A.E. and J.N. Grossman (1987) *Meteoritics* 22, 237-251. [17] P. Srinivasan, et al. (2013) *LPSC XLIV*. [18] Chistofersen, et al., (2012) *LPSC XLV*. [19] Tait, A. et al (this meeting).